

Published in final edited form as:

Nat Struct Mol Biol. ; 18(10): 1139–1146. doi:10.1038/nsmb.2115.

Weak Seed-Pairing Stability and High Target-Site Abundance Decrease the Proficiency of *Isy-6* and Other miRNAs

David M. Garcia^{1,2,3,8}, Daehyun Baek^{1,2,3,4,5,8}, Chanseok Shin^{1,2,3,6}, George W. Bell¹, Andrew Grimson^{1,2,3,7}, and David P. Bartel^{1,2,3}

¹Whitehead Institute for Biomedical Research, Cambridge, Massachusetts, USA

²Howard Hughes Medical Institute

³Department of Biology, Massachusetts Institute of Technology, Cambridge, MA, USA

⁴School of Biological Sciences, Seoul National University, Seoul, Republic of Korea

⁵Bioinformatics Institute, Seoul National University, Seoul, Republic of Korea

⁶Department of Agricultural Biotechnology, Seoul National University, Seoul, Republic of Korea

Abstract

Most metazoan microRNAs (miRNAs) target many genes for repression, but the nematode *Isy-6* miRNA is much less proficient. Here, we show that the low proficiency of *Isy-6* can be recapitulated in HeLa cells and that miR-23 (a mammalian miRNA) also has low proficiency in these cells. Reporter results and array data both indicate two properties of these miRNAs that impart low proficiency: their weak predicted seed-pairing stability (SPS) and their high target-site abundance (TA). These two properties also explain differential propensities of small interfering RNAs (siRNAs) to repress unintended targets. Using these insights, we expand the TargetScan tool for quantitatively predicting miRNA regulation (and siRNA off-targeting) so as to model differential miRNA (siRNA) proficiencies, thereby improving prediction performance. Moreover, we propose that siRNAs designed to have both weaker SPS and higher TA will have fewer off-targets without compromised on-target activity.

Introduction

MicroRNAs are ~22-nucleotide RNAs that pair to the messages of protein-coding genes to direct posttranscriptional repression of these target mRNAs^{1,2}. In animals, numerous studies using a wide range of methods, including comparative sequence analysis, site-directed mutagenesis, genetics, mRNA profiling, co-immunoprecipitation, and proteomics, have repeatedly shown that perfect pairing to miRNA nucleotides 2–7, known as the miRNA seed, is important for the recognition of many if not most miRNA targets³. To impart more than marginal repression of mammalian targets, this seed pairing is usually augmented by either a match to miRNA nucleotide 8 (7mer-m8 site)^{4–7} or an A across from nucleotide 1

Correspondence should be addressed to D.P.B. (dbartel@wi.mit.edu) and D.B. (baek@snu.ac.kr).

⁷Present address: Department of Molecular Biology and Genetics, Cornell University, Ithaca, New York, USA.

⁸These authors contributed equally to this work.

Author Contributions

D.M.G. performed most reporter assays and associated experiments and analyses. D.B. performed all the computational analyses except for reporter analyses. G.W.B. implemented revisions to the TargetScan site. C.S. and A.G. performed assays and analyses involving miR-23. D.M.G., D.B. and D.P.B. wrote the paper.

Competing Financial Interests

The authors declare no competing financial interests.

(7mer-A1 site)^{4,7} or by both (8mer site)^{4,7}. In relatively rare instances, targeting also occurs through 3'-compensatory sites^{4,5,8} and centered sites⁹, for which substantial pairing outside the seed region compensates for imperfect seed pairing.

A single miRNA can target hundreds of distinct mRNAs through seed-matched sites¹⁰. Indeed, most human mRNAs are conserved regulatory targets⁸, and many additional regulatory interactions occur through nonconserved sites¹¹⁻¹³. However, not every site is effective; 8-nucleotide sites are more often effective than 7-nucleotide sites, which are more often effective than 6-nucleotide sites^{7,14}. Another factor is site context. For example, sites in the 3'UTRs are more often effective than those in the path of the ribosome⁷. Among 3'UTR sites, those away from the centers of long UTRs and those within high local A-U sequence context are more often effective⁷, consistent with reports that sites predicted to be within more accessible secondary structure tend to be more effective¹⁵⁻¹⁹. Also influencing site efficacy is proximity to other miRNA-binding sites^{7,20}, to protein-binding sites²¹, and to sequences that can pair to the 3' region of the miRNA, particularly nucleotides 13-17 (ref 7).

Studies of site efficacy have focused primarily on different sites to the same miRNA, without systematic investigation of whether some miRNA sequences might be intrinsically more proficient at targeting than others. Broadly conserved miRNAs typically have many more conserved targeting interactions than do other miRNAs^{4,8}, and highly or broadly expressed miRNAs appear to target more mRNAs than do others²², but these phenomena reflect evolutionary happenstance more than intrinsic targeting proficiency.

Our interest in targeting proficiency was spurred by intriguing results regarding the *lcy-6* miRNA. When tested in *C. elegans*, only one of 14 predicted targets with 7-8-nucleotide seed-matched sites responds to *lcy-6*, which was interpreted to show that perfect seed-pairing is not a generally reliable predictor for miRNA-target interactions²³. An alternative interpretation, which seemed more parsimonious with findings for many other miRNAs in other contexts³, is that the results for *lcy-6* might not be generally applicable to other miRNAs because *lcy-6* might have unusually high targeting specificity because of unusually low targeting proficiency. A similar rationale might explain results for mammalian miR-23, another miRNA that confers unusually weak responses from most reporters designed to test predicted targets.

When considering properties that might confer a low targeting proficiency, we noted that both *lcy-6* and miR-23 have unusually AU-rich seed regions, which could lower the stability of seed-pairing interactions. Perhaps a threshold of seed-pairing stability (SPS) is required for the miRNA to remain associated with targets long enough to achieve widespread seed-based targeting. Indeed, predicted SPS correlates with the propensity of siRNAs to repress unintended targets²⁴, a process called "off-targeting," which occurs through the same seed-based recognition as that for endogenous miRNA targeting¹⁰. Potentially confounding this interpretation, however, was that miRNAs with AU-rich seed regions have more 3'UTR binding sites, a consequence of the AU-rich nucleotide composition of 3'UTRs, which could dilute the effect on each target message. Indeed, target-site abundance (TA) can be manipulated to titrate miRNAs away from their normal targets^{25,26}, and natural TA has been proposed to play a role in miRNA targeting and siRNA off-targeting^{27,28}, although these reported TA effects have not been fully disentangled from potential SPS effects. Here, we find that both SPS and TA have a substantial impact on targeting proficiency, and then apply these insights to improve miRNA target predictions.

Results

The targeting specificity of *Isy-6* is recapitulated in HeLa cells

Isy-6 targeting was originally examined in a *C. elegans* neuron, whereas the more proficient targeting by other miRNAs was experimentally demonstrated in other systems, sometimes in vertebrate tissues or primary cells^{11,13,29,30} but more often in cell lines³. To test whether differences in targeting proficiency might be attributed to the very different biological contexts in which the miRNAs had been examined, we ported the 14 3'UTRs tested in *C. elegans* into a luciferase reporter system typically used in mammalian cell lines and introduced the *Isy-6* miRNA by co-transfecting an imperfect RNA duplex representing the miRNA and miRNA* sequences (Supplementary Fig. 1a). As observed in worms, only the *cog-1* 3'UTR responded in HeLa cells (Fig. 1b). Repression was lost when a control miRNA (miR-1) replaced *Isy-6* or when the two *cog-1* sites were mutated, introducing either mismatches (Fig. 1b) or G:U wobbles (Supplementary Fig. 1b,c)

Each of the 14 3'UTRs had at least one canonical 7–8-nucleotide *Isy-6* site, and 11 UTRs had a site conserved in three sequenced nematodes (Supplementary Table 1). When evaluated using the context-score model, some sites had scores comparable to those of sites that mediate repression in this assay⁷ (Supplementary Table 1). Moreover, the C27H6.9 3'UTR had two 8mer sites with scores matching those of the two *cog-1* sites. The close match between the results in our heterologous reporter assay and previous results in *C. elegans* neurons indicated that the exquisite specificity for targeting the *cog-1* 3'UTR did not require the endogenous cellular context of *Isy-6* repression; it was operable in HeLa cell culture and thereby attributable to the intrinsic properties of *Isy-6* and its targets. This unifying result also implied that these properties could be investigated in mammalian cell culture, which is easier than using stable reporter lines in worms.

Increasing SPS while decreasing TA elevates targeting proficiency

As expected for a miRNA with sequence UUUGUAU at nucleotides 2–8, the calculated free energy (ΔG°) of the predicted SPS for the *Isy-6* 8mer or 7mer-m8 sites (both seven base pairs) was $-3.65 \text{ kcal mol}^{-1}$, which was weaker than that of all but one conserved nematode miRNA (Fig. 1c). The *Isy-6* predicted SPS was also weaker than that of the weakest of 87 broadly conserved vertebrate miRNAs (Fig. 1d). The predicted ΔG° of an 8mer or 7mer-m8 seed match for miR-23 was $-5.85 \text{ kcal mol}^{-1}$, which fell in the bottom quintile for broadly conserved vertebrate miRNAs (Fig. 1d). Similar results are observed for 7mer-A1 or 6mer sites (both 6 base pairs) for both miRNAs (Supplementary Fig. 1d,e).

Isy-6 also falls at the extreme end of the distribution of TA for miRNAs in nematodes and human (Fig. 1e, f). To predict the TA in a genome, we counted the number of sites in a curated set of distinct 3'UTRs. When considering a particular cell type, the genome TA was converted to a transcriptome TA by considering the relative levels of each mRNA bearing a site, although in practice the genome and transcriptome TA levels were highly correlated. For example, the transcriptome TA for HeLa cells (TA_{HeLa}) correlated nearly perfectly with the genome TA ($R^2 = 0.98$, $P < 10^{-100}$, Spearman's correlation test, Supplementary Fig. 1f). When considering 8mer and 7mer-m8 sites (which both pair to nucleotides 2–8), *Isy-6* had a genome TA that ranked 2nd among 60 *C. elegans* miRNA families and a TA_{HeLa} that would place it beside miR-23, which ranks 5th among the 87 vertebrate families (Fig. 1e and Supplementary Fig. 1g).

To test the hypothesis that either the weak SPS or the high TA of *Isy-6* influences its targeting proficiency, we made three substitutions in the *Isy-6* seed that changed both properties. The three substitutions converted the *Isy-6* seed to that of miR-142-3p (Fig. 1a; Supplementary Fig. 1a), which changed the predicted SPS to $-7.70 \text{ kcal mol}^{-1}$, which was

–4.05 kcal mol⁻¹ stronger than that of *Isy-6* and near the median values for conserved nematode and vertebrate miRNAs (Fig. 1c, d). The substitutions also changed the predicted TA to 10^{2.957} sites in *C. elegans* and 10^{3.207} sites in human, values below the median of conserved miRNAs in both genomes (Fig. 1e, f). When assayed using reporters with compensatory substitutions in their seed matches, co-transfecting this miR-142/*Isy-6* chimeric miRNA repressed nine of 14 reporters, a fraction within, if not exceeding, the range expected in this system when using reporters with the site types and contexts assayed (Fig. 1g). Repeating the experiment using the full-length miR-142-3p sequence (Fig. 1a; Supplementary Fig. 1a) gave similar results, indicating that miRNA sequence outside the seed region was irrelevant for repression of both the *cog-1* 3'UTR and the other *C. elegans* 3'UTRs (Fig. 1h).

Like *Isy-6*, miR-23 also had low targeting proficiency in our system. A survey of 17 human 3'UTR fragments, randomly chosen from a set with two 7–8-nucleotide miR-23 sites (conserved or nonconserved) spaced within 700 nt of each other, found only one fragment to be repressed by miR-23 endogenous to either HeLa or HepG2 cells (data not shown). Subsequent experiments focusing on the six UTRs with the most favorable context scores (Supplementary Table 1) showed that co-transfecting additional miR-23a imparted marginal if any repression (Fig. 1i).

To test if increasing SPS while decreasing TA might also improve the targeting proficiency of miR-23a, we converted two A:U seed pairs into two G:C pairs (Fig. 1a; Supplementary Fig. 1a), which boosted the predicted SPS from –5.85 kcal mol⁻¹ to –8.67 kcal mol⁻¹ while reducing the TA from the 5th highest of the 87 vertebrate families to below the lowest. When assaying this miRNA, called miR-CGCG, using reporters with compensatory substitutions in their seed matches, the sporadic and marginal repression observed with the wild-type UTRs became much more robust (Fig. 1j). These results indicated that miR-23a had low targeting proficiency because of either its weak SPS or its high TA, or both, thereby extending our findings to a mammalian miRNA and mammalian 3'UTRs.

Separating the effects of SPS and TA on miRNA targeting

To begin to differentiate the potential effects of SPS from those of TA, we considered the relationship between these two properties for all 16,384 possible heptamers. When examining the *C. elegans* 3'UTRs, these properties were highly anti-correlated (Fig. 2a, $R^2 = 0.680$, $P < 10^{-100}$, Spearman's correlation test). When examining mammalian 3'UTRs the relationship was still highly significant, but the substantial depletion of CG dinucleotides in the vertebrate transcriptome³¹ created more spread in TA, which lowered correlation coefficients for both human (Fig. 2b, $R^2 = 0.121$, $P < 10^{-100}$) and mouse (Supplementary Fig. 2a, $R^2 = 0.081$, $P < 10^{-100}$). In general, each additional CG dinucleotide imparted an additional log₁₀ reduction in TA.

To test the influence of TA on *Isy-6* targeting proficiency, we designed the low-TA (LTA) version of *Isy-6*, which had two point substitutions in the *Isy-6* seed (Fig. 2c; Supplementary Fig. 1a). Substituting U4 with a C (substitution U4C) introduced a CG dinucleotide, whereas the other substitution, U2A, facilitated later investigation of SPS. Because of the CG dinucleotide, LTA-*Isy-6* had a predicted TA_{HeLa} 95% lower than that of *Isy-6*, a value that would be 3rd lowest among the conserved vertebrate miRNA families. Although the substitutions also increased SPS, the predicted SPS of –5.49 kcal mol⁻¹ was still slightly weaker than that of miR-23 and well below the median for both nematode and vertebrate conserved miRNAs (Fig. 1c, d). When assayed using reporters with compensatory substitutions in their seed matches, LTA-*Isy-6* repressed the *cog-1* reporters and only three others (Fig. 2d). Two (F55G1.12 and C27H6.9) were repressed only marginally (<1.3 fold), which was reminiscent of the marginal repression imparted by miR-23 when using its

cognate sites, and for the third, T20G5.9, much of the apparent repression was attributed to normalization to the miR-1 results, which in the case of this UTR were unusual (Supplementary Fig. 2d). Taken together, the LTA-*Isy-6* results indicated that lowering TA was not sufficient on its own to confer robust targeting proficiency.

To increase SPS without changing TA, we replaced each of the two seed adenines of LTA-*Isy-6* with 2,6-di-aminopurine (DAP or D). DAP is an adenine analog with an exocyclic amino group at position 2, which enables it to pair with uracil with geometry and thermodynamic stability resembling that of a G:C pair (Fig. 2e). Because nearest-neighbor parameters had not been determined for model duplexes containing D:U pairs, we estimated SPS using the values for A:U pairs and adding $-0.9 \text{ kcal mol}^{-1}$ for each D:U pair, as this is the value attributed to an additional hydrogen bond in model duplexes³². With this approximation, the D-LTA-*Isy-6* miRNA had a predicted SPS of $-7.29 \text{ kcal mol}^{-1}$, which approached $-7.87 \text{ kcal mol}^{-1}$, the median predicted SPS of the conserved vertebrate miRNAs. When assayed using the same reporters as used for LTA-*Isy-6*, D-LTA-*Isy-6* repressed seven of fourteen reporters (Fig. 2f). Although less proficient than that observed with the miR-142 seed (Fig. 1g, h), repression was greater than that observed for LTA-*Isy-6* and on par with that expected for mammalian miRNAs in this system when using reporters with the site types and site contexts assayed.

We next tested D-miR-23, which also had two seed adenines replaced by DAP, thereby boosting the predicted SPS from $-5.85 \text{ kcal mol}^{-1}$ to $-7.65 \text{ kcal mol}^{-1}$. Five of the six reporters with miR-23 sites were repressed significantly greater by D-miR-23a than by wild-type miR-23a (Fig. 2g), thereby demonstrating a favorable effect for increasing SPS in the context of very high TA (93rd percentile). However, repression was still considerably lower than that conferred by miR-CGCG, presumably because miR-CGCG had lower TA and somewhat stronger SPS ($-8.67 \text{ kcal mol}^{-1}$), although we cannot exclude the possibility that the non-natural DAP in the miRNA compromised activity.

In summary, the results with DAP-substituted miRNAs show that for miRNAs with weak SPS, increasing SPS can enhance targeting proficiency, regardless of whether these miRNAs have high or low TA. Because DAP-substitution changed the predicted SPS without changing the sites in the UTRs, these results indicated that the low proficiency was due to weak SPS rather than occlusion of the sites by RNA-binding proteins that recognized the miRNA seed matches. Taken together, our reporter results also suggest that lowering TA can further enhance targeting proficiency, particularly for miRNAs with moderate-to-strong SPS.

Global impact of TA and SPS on targeting proficiency

To examine the global impact of TA and SPS on targeting, we collected 175 published microarray datasets that monitored the response of transfecting miRNAs or siRNAs (sRNAs) into HeLa cells (Supplementary Table 2). Datasets reporting the effects of sRNAs with the same seed region were combined, yielding results for 102 distinct seeds that covered a broad spectrum of TA and predicted SPS (Fig. 3a). For each of these 102 datasets, we determined the mean repression of mRNAs with a single 3' UTR 8mer site and no other sites in the message, and plotted these values with respect to both the TA_{HeLa} and predicted SPS of the transfected sRNA (Fig. 3b, top). sRNAs with lower TA_{HeLa} were more effective than those with higher TA_{HeLa} , and those with stronger predicted SPS were more effective than those with weaker predicted SPS ($P=0.0006$ and 0.0054 for TA_{HeLa} and SPS, respectively, Pearson's correlation test; Table 1). When using multiple linear regression to account for the cross-correlation between TA_{HeLa} and SPS, correlations were still at least marginally significant for the individual features ($P=0.005$ and 0.05 , t test; Table 1), which indicated that both properties were independently associated with the proficiency of

targeting 3'UTR sites. Similar results were observed for targeting 7mer-m8, 7mer-A1, and 6mer sites (Fig. 3b and Table 1).

Although both TA and SPS each significantly influenced targeting proficiency, together they explained only a minority of the variability (Table 1). Most of the variability might be from factors unrelated to targeting, such as array noise, differential transfection efficiencies, or differential sRNA loading or stability. To reduce variability from these sources, we focused on 74 datasets for which responsive messages were significantly enriched in 3'UTR sites to the transfected sRNA (Fig. 3a, red squares; Supplementary Table 2). With these filtered datasets, correlations between proficiency and both TA_{HeLa} and SPS were stronger and observed with similar statistical significance, even though the filtering reduced the quantity of data analyzed and might have preferentially discarded datasets for which high TA or weak SPS prevented detectable repression (Supplementary Fig. 3a,b and Supplementary Table 3).

Studies monitoring global effects of miRNAs on target repression have concluded that sites in open reading frames (ORFs) can mediate repression but that the efficacy of these sites is generally less than that of sites in 3'UTRs^{7,30,33,34}. To examine the impact of TA and SPS on targeting in ORFs, we considered expressed messages that had a single ORF site but no additional sites in the rest of the message. For 7mer-m8 and 6mer sites, mean repression significantly correlated with both TA_{HeLa} and predicted SPS, and for the other two sites in ORFs, mean repression significantly correlated with TA_{HeLa} (Fig. 3c and Table 1). The response of sites in 5'UTRs did not significantly correlate with either TA or predicted SPS (Table 1), consistent with the idea that 5'UTRs harbor relatively few effective sites³.

We next examined the quantitative impact of TA and SPS on targeting proficiency. The same sets of mRNAs with single sites to the cognate sRNAs were considered, and for each site type and each mRNA region, mRNAs were binned into quartiles ranked by either low TA or strong predicted SPS. For each site type, messages in the top quartile responded more strongly than those in the bottom (Fig. 3d). The differences usually were substantial. For example, repression of the top quartile of mRNAs with 7mer-A1 sites matched the mean repression of mRNAs with 7mer-m8 sites, whereas repression of the bottom quartile resembled the mean repression of mRNAs with 6mer sites.

Improved miRNA target prediction

One of the more effective tools for mammalian miRNA target prediction is the context score³⁰. Context scores are used to rank mammalian miRNA target predictions by modeling the relative contributions of previously identified targeting features, including site type, site number, site location, local AU content, and 3'-supplementary pairing, to predict the relative repression of mRNAs with 3'UTR sites⁷. However, the context-score model was not designed to consider differences between sRNAs, such as TA or SPS, which can cause sites of one miRNA to be more robustly targeted compared to those of another (assuming equal expression of the two miRNAs).

To build a model appropriate for predicting the relative response of targets of different miRNAs, we considered TA and SPS as two independent variables when performing multiple linear regression on the 11 microarray datasets used previously for the initial development and training of the context-score model⁷. The other parameters were local A-U content, the location of the site within the 3'UTR, and 3'-supplementary pairing⁷. For each site type, TA and/or SPS robustly contributed (Supplementary Table 4). The scores generated by these models were called context+ scores, because they consider site type and context plus sRNA proficiency. We then generated the total context+ score for each mRNA

with 3'UTR sites, relying on the observation that multiple sites typically act independently with respect to each other⁷.

The predictive value of the new model was tested using data from array datasets not used to train the model, comparing the performance of the predicted targets ranked using the total context+ scores to those ranked using scores of the original model. To examine if any improvement over the original model was from training the model with multiple linear regression rather than simple linear regression, we also used multiple linear regression to build a model that considered only the three parameters used to build the original model (context-only scores, Supplementary Table 5). For each model, predicted targets with 7–8-nucleotide sites were ranked by score and assigned to 10 bins. The context+ scores performed better than the old context scores at predicting the response to the sRNAs (Fig. 4a), yielding significantly stronger mean repression for the top two bins ($P = 5 \times 10^{-56}$ and 3×10^{-8} for bins 1 and 2, respectively) and significantly weaker repression in the bottom four bins ($P = 6 \times 10^{-10}$, 1.5×10^{-5} , 1×10^{-7} , and 3×10^{-4} for bins 7, 8, 9, and 10, respectively, Wilcoxon's rank sum test). Improved specificity was also illustrated in ROC curves (Supplementary Fig. 4a).

Because most 6mer sites and ORF sites are either nonresponsive or only marginally responsive to the miRNA, algorithms that achieve useful prediction specificity do so at the expense of ignoring these sites³. Having found that low TA and strong SPS correlated with substantially greater efficacy of these marginal sites (Fig. 3c, d), we extended the context+ scores to 6mer sites. For the context+ model, the top bin of mRNAs with 6mer 3'UTR sites but no larger sites (Fig. 4b) had average repression resembling that observed for the third bin of mRNAs with 7–8-nucleotide 3'UTR sites (Fig. 4a; ROC curves, Supplementary Fig. 4b). Context-only and context+ scores were also generated for ORF sites, changing only the parameter of site location, which was not applicable for ORF sites because it accounts for the lower efficacy of sites near the middle of long 3'UTRs⁷. In ORFs, we found that sites further from the stop codon tended to be less effective, and thus the distance from the stop codon (linearly scaled distance of 0 to 1500 nt) was included as a parameter. Although this context+ model was not substantially better than the context-only model for ORF sites (perhaps because data from only 11 miRNAs were used in the regression), both models had predictive value. When comparing mRNAs with at least one 8mer ORF site (Fig. 4c), those ranked in the top bin had average repression resembling that observed for the second or third bins of mRNAs with 7–8-nucleotide 3'UTR sites (Fig. 4a).

Overall, our findings showed that taking TA and SPS into account could significantly improve miRNA target prediction when pooling results from multiple sRNAs. Training on the 11 miRNA transfection datasets that had been used for the original context scores was appropriate for demonstrating the improvement that could be achieved by taking TA and SPS into account. We reasoned, however, that training on the 74 filtered datasets could generate a more precise context+ model to be used to quantitatively predict repression. As expected, correlations for all four parameters had even greater statistical significance when training the model on more data (Supplementary Table 6). Although an SVM (support vector machine) approach should in principle yield even better results by capturing effects lost in multiple linear regression due to multicollinearity, enhanced performance was not observed with SVM (Supplementary Fig. 4c–e). Therefore, we used multiple linear regression because it enabled more convenient calculation of context+ scores (Supplementary Fig. 5a). We will use these new scores in version 6.0 of TargetScan (targetscan.org).

Additional Considerations

A caveat of the reporter experiments was that miRNA sequence changes designed to alter TA or SPS might have inadvertently influenced other factors, such as miRNA stability or its loading into the silencing complex. However, our computational analyses of 102 array datasets also showed that TA and SPS each independently influence targeting efficacy. Therefore, if differences in sRNA stability or loading have confounded interpretation of our results, these differences must correlate with either predicted SPS or TA. Analysis of published miRNA over-expression data countered this possibility, revealing no correlation between miRNA accumulation and predicted SPS or TA (Supplementary Fig. 3c,d). Furthermore, experiments examining the RNAs co-purifying with AGO2 indicated that the difference in proficiency observed between *lgy-6* and miR-142/*lgy-6* was not merely attributable to less accumulation of *lgy-6* in the silencing complex (Supplementary Fig. 1m–s).

Discussion

The correlation between strong SPS and low TA confounded previous efforts to examine the influence of these parameters on targeting efficacy, with one study implicating SPS and not TA²⁴, and others implicating TA and not SPS^{27,28}. Our results indicated that both parameters influence efficacy and solved one of the mysteries in miRNA targeting: the failure of *lgy-6* to repress all but one of the 14 examined seed-matched mRNAs. Previous solutions hypothesized that the seed-based targeting model is unreliable²³, or that sites of the 13 non-responsive mRNAs fall in inaccessible UTR structure¹⁸. Our work shows that the actual solution is the unusually weak SPS and high TA of the *lgy-6* miRNA. Changing these parameters to resemble those of more typical miRNAs imparted typical seed-based targeting proficiency, even though the sites were in their original UTR contexts, thereby demonstrating that neither the reliability of seed-based targeting nor the accessibility of the sites were at issue.

MicroRNAs with unusually weak predicted SPS and unusually high TA, such as miR-23 and *lgy-6*, appear to have relatively few targets. Indeed, *lgy-6* might have only a single biological target, the *cog-1* mRNA—an extreme exception to the well-supported finding that metazoan miRNAs generally have dozens if not hundreds of preferentially conserved targets^{4,8,35,36}. Solving the mystery of why so few mRNAs respond to *lgy-6* brings to the fore a second mystery, still unsolved: How is the *cog-1* 3'UTR so efficiently recognized and repressed by a miRNA with such weak targeting proficiency? This UTR has two 8mer sites, which by virtue of their conservation make *cog-1* the top predicted target of *lgy-6* (ref. ³), but this is only part of the answer³⁷. Improving the context-score model to take into account the differential SPS and TA of different miRNAs will help focus attention on the predicted targets of miRNAs with more typical proficiencies, but leaves unsolved the problem of how to predict the few biological sites of the less proficient miRNAs without recourse to considering site conservation.

MicroRNAs with very high TA, such as *lgy-6* or miR-23, and those with very low TA, such as miR-100 or miR-126, two broadly conserved vertebrate miRNAs containing CG dinucleotides in their seeds (Supplementary Table 7), appear to represent two strategies for targeting very few genes, accomplished at opposite ends of the TA spectrum. For miRNAs with very high TA, other UTR features flanking the seed sites are required for regulation, as illustrated for *lgy-6* regulation of *cog-1* (ref. ³⁷), whereas miRNAs with very low TA simply have far fewer potential target sites to begin with.

Our results also have implications for how siRNA might be designed to reduce off-targets. Previous studies have proposed that off-targets could be reduced by designing siRNAs with

low TA²⁷ or weak SPS²⁴, and our results implied that off-targets could be largely eliminated by designing siRNAs with both high TA and weak SPS. One concern, though, is that such siRNAs might also be ineffective at recognizing the desired mRNA target because pairing to this target would nucleate on a match with weak SPS and might be titrated by the many other mRNAs with seed matches. To investigate this concern, we examined a published dataset of high-throughput luciferase assays reporting the response to 2,431 different siRNAs³⁸. siRNAs with weak predicted SPS knocked down the desired target more effectively than did those with strong predicted SPS (Fig. 4d; $P = <10^{-100}$, Pearson's correlation test), presumably because of preferential loading into the silencing complex^{39,40}. Moreover, high TA did not compromise the desired targeting efficacy, even after correcting for the cross-correlation between TA and SPS ($P = 0.16$, Pearson's correlation test). Therefore, designing siRNAs with high TA and weak SPS should minimize off-target effects without compromising knockdown of the desired target.

Highly expressed mRNAs tend to be evolutionarily depleted in sites for co-expressed miRNAs, a phenomenon partly attributed to the possibility that these mRNAs might otherwise titrate the miRNAs from their intended targets^{12,41,42}. Titration can also provide a useful mechanism for cells to regulate miRNA activity, as illustrated by *IPS1* titration of miR-399 in *Arabidopsis*²⁵. Beneficial titration has even been proposed to explain why so many miRNA sites are conserved⁴³. However, because most preferentially conserved sites fall in lowly-to-moderately expressed mRNAs, and because these sites each comprise only a tiny fraction of the TA, each could impart at most a correspondingly tiny effect on the effective miRNA concentration—much less than that required to selectively retain the site. A though titration functions cannot explain most site conservation, TA could be dynamic during development, with interesting consequences. For example, the increase of a miRNA during development will often be accompanied by a decrease in its transcriptome TA, a consequence of the evolutionary depletion of sites in mRNAs co-expressed at high levels with the miRNA^{12,42}. This accompanying TA decrease would sharpen the transition between the non-repressed and repressed states of targets.

When predicting SPS we used parameters derived from model RNA duplexes, which presumably underestimated the actual affinity of RNA segments pairing to Argonaute-bound seed regions^{2,3,44,45}. The extent to which Argonaute enhances affinity might vary for different seed sequences. These potential differences, however, did not obscure our detection of an influence of SPS on targeting proficiency. Thus, our study provided a lower bound on the actual influence of SPS, as well as an approach for learning its full magnitude once accurate SPSs of Argonaute-bound complexes are known.

Methods

Reporter assays

For *Isy-6* reporter assays, HeLa cells were plated in 24-well plates at 5×10^4 cells per well. After 24 hours, each well was transfected with 20 ng TK-*Renilla*-luciferase reporter (pIS1)⁴⁶, 20 ng firefly-luciferase control reporter (pIS0)⁴⁶, and 25 nM miRNA duplex (Dharmacon) (Supplementary Fig. 1a), using Lipofectamine 2000 (Invitrogen). For miR-23 reporter assays, conditions were the same except for transfected DNA: 10 ng SV40-*Renilla*-luciferase reporter (pIS2)⁴⁶, 25 ng firefly-luciferase control reporter (pIS0), 1.25 μ g pUC19 carrier DNA. Luciferase activities were measured 24 hours after transfection with the Dual-Luciferase Assay (Promega) and a Veritas microplate luminometer (Turner BioSystems). For every construct assayed, four independent experiments, each with three biological replicates, were performed. To control for transfection efficiency, firefly activity was divided by *Renilla* activity. *Renilla* values for constructs with sites matching the cognate miRNA were then normalized to the geometric mean of values for otherwise identical

constructs in which the sites were mutated. To control for differences not attributable to the cognate miRNA, the ratios were further normalized to ratios for the same constructs tested with a non-cognate miRNA, miR-1. These double-normalized results are presented in the main figures; singly normalized results are presented in Supplementary Figures 1h–l and 2d–f.

Constructs

3'UTRs of *Isy-6* predicted targets²³ were subcloned into XbaI and EagI sites in pIS1, and 3'UTRs of miR-23 predicted targets were cloned into SacI and SpeI sites in pIS2 after amplification (UTR sequences, Supplementary Table 1). Mutations were introduced using Quikchange (Stratagene) and confirmed by sequencing.

Predicted SPS

SPS was predicted using nearest-neighbor thermodynamic parameters, including the penalty for terminal A:U pairs³². The contribution of the A at position 1 of 8mer and 7mer-A1 sites was not included because this A does not pair to the miRNA⁴ and thus its contribution is not expected to differ in a predictable way for different miRNAs. When performing linear regression analyses, the predicted SPS of positions 2–8 was used for 8mer and 7mer-m8 sites, and the predicted SPS of positions 2–7 was used for 7mer-A1 and 6mer sites. When assigning a single value for 7–8-nucleotide sites (7mer-A1, 7mer-m8, and 8mer), a mean weighted value of the three site types was used. This mean SPS was calculated as $[(6\text{mer SPS})(7\text{mer-A1 TA}) + (7\text{mer-m8 SPS})(7\text{mer-m8 TA} + 8\text{mer TA})] \div (7\text{mer-A1 TA} + 7\text{mer-m8 TA} + 8\text{mer TA})$.

Reference mRNAs

To generate a list of unique mRNAs, human full-length mRNAs obtained from RefSeq⁴⁷ and H-Invitational⁴⁸ databases were aligned to the human genome⁴⁹ (hg18) using BLAT⁵⁰ software and processed as described to represent each gene by the mRNA isoform with the longest UTR³⁰. These unique full-length mRNAs, which were each represented by the genomic sequence of their exons (since the genomic sequence was of higher quality than the mRNA sequence), were the “reference mRNAs” (Supplementary Table 8). Mouse full-length mRNAs were obtained from RefSeq⁴⁷ and FANTOM DB⁵¹ databases, aligned against the mouse genome⁵² (mm9), and processed similarly. For *C. elegans* and *D. melanogaster*, we obtained 3'UTR sequences from TargetScan (targetscan.org)^{22,53}. Mature miRNA sequences were downloaded from the miRBase web site⁵⁴.

Microarray processing and mapping to reference mRNAs

We collected published datasets reporting the response of HeLa mRNAs 24 hours after 100 nM sRNA transfection using Agilent arrays (two-color platform), excluding datasets for which either multiple sRNAs were simultaneously transfected or the transfected RNAs contained chemically modified nucleotides (Supplementary Table 2). If probe sequences for an array platform were available, they were mapped to genomic locations in the human genome using BLAT⁵⁰ software. For some arrays (e.g., GSE8501), probe sequences were unavailable, but associated cDNA or EST sequence IDs were available. In such cases, genomic coordinates of cDNAs and ESTs obtained from the UCSC Genome Browser⁵⁵ were used as if they were coordinates of array probes. Each probe and its associated mRNA fold-change value were mapped to the reference mRNA sharing the greatest overlap with the probe's genomic coordinates, 15 bases. When multiple probes were mapped to a single reference mRNA, the median fold change was used. To avoid analysis of mRNAs not expressed in HeLa cells, only mRNAs with signal above the median in the mock-transfection samples were considered. For each array, the median fold change of reference

mRNAs without any 6–8-nucleotide site was used to normalize the fold changes of all reference mRNAs. To correct for the global association between mRNA fold change and AU content of the mRNA transcript, the LOWESS filtering was applied by using `malowess()` function within MATLAB (Supplementary Table 9). For some arrays, the transfected sRNA is designed to target nearly perfectly matching (18 nucleotides) mRNAs, in which case, these intended targets were excluded from analysis.

Motif-enrichment analysis for array filtering

To evaluate array datasets, we performed motif-enrichment analysis using the Fisher's exact test for a 2×2 contingency table, populated based on whether the reference mRNA had a 7mer motif for the cognate sRNA in its 3' UTR and whether it was among the top 5% most down-regulated mRNAs. If multiple arrays examined the effects of transfecting sRNAs with identical seed regions (positions 2–8), the P value of the Fisher's exact test for site enrichment (considering either of the two 7mer sites and picking the one with the lower P value) was assessed for each array, and the array with the median P value was chosen to represent that seed region, yielding 102 representative arrays (Supplementary Table 2). To obtain a filtered dataset, this test was reiterated for the 16,384 7mers, and arrays were retained if the motif most significantly associated with down-regulation was the 7mer-m8 or 7mer-A1 site of the transfected sRNA; 74 arrays passed this filter (Supplementary Table 2). Results of multiple linear regression and other analyses were robust to cutoff choice (other cutoffs tested, 10, 15, and 20%; data not shown).

TA

TA in the human transcriptome was calculated as the number of non-overlapping 3' UTR 8mer, 7mer-m8, and 7mer-A1 sites in the reference mRNAs. An analogous process was used to calculate TA in mouse, *C. elegans*, and *D. melanogaster*. To calculate TA_{HeLa} , each site was weighted based on mRNA-Seq data³³. Predicted SPS and TA values for all heptamers in *C. elegans*, human and HeLa, mouse, and *D. melanogaster* are provided in Supplementary Table 10.

miRNA target prediction and analysis of siRNA efficacy

Context scores were calculated for the cognate sites of the reference mRNAs using the simple linear-regression parameters reported previously⁷. Prior to fitting, scores for each parameter were scaled from 0 to 1 (Supplementary Fig. 5b). To account for site type without the complication of multiple sites, models were developed for each type individually, using mRNAs with only a single site to the cognate miRNA (Supplementary Fig. 5c). The multiple linear regression models for context-only and context+ were computed by using `lm()` function in the R package version 2.11.1

Supplementary Material

Refer to Web version on PubMed Central for supplementary material.

Acknowledgments

We thank Dominic Didiano and Oliver Hobert (Columbia University) for *Isy-6* target constructs, Vincent Auyeung, Robin Friedman, Calvin Jan, and Huili Guo for helpful discussions and for sharing datasets prior to publication. This work was supported by an NIH grant GM067031 (D.P.B) and a Research Settlement Fund for the new faculty of SNU (D.B.). D.P.B. is an investigator of the Howard Hughes Medical Institute.

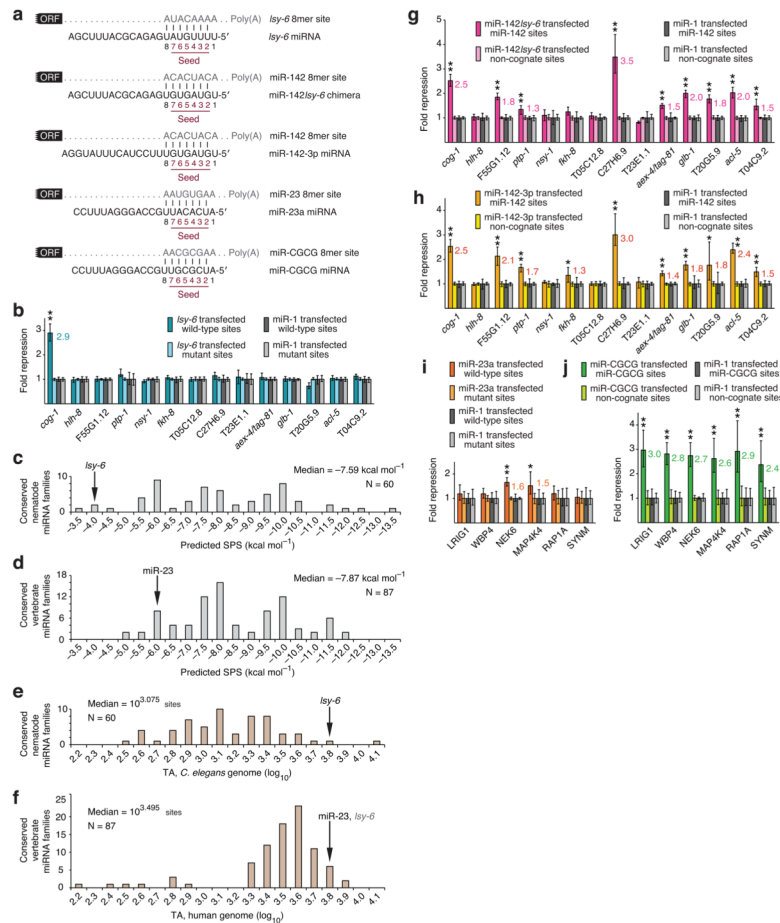
References

1. Ambros V. The functions of animal microRNAs. *Nature*. 2004; 431:350–5. [PubMed: 15372042]

2. Bartel DP. MicroRNAs: genomics, biogenesis, mechanism, and function. *Cell*. 2004; 116:281–97. [PubMed: 14744438]
3. Bartel DP. MicroRNAs: target recognition and regulatory functions. *Cell*. 2009; 136:215–33. [PubMed: 19167326]
4. Lewis BP, Burge CB, Bartel DP. Conserved seed pairing, often flanked by adenosines, indicates that thousands of human genes are microRNA targets. *Cell*. 2005; 120:15–20. [PubMed: 15652477]
5. Brennecke J, Stark A, Russell RB, Cohen SM. Principles of microRNA-target recognition. *PLoS Biol*. 2005; 3:e85. [PubMed: 15723116]
6. Krek A, et al. Combinatorial microRNA target predictions. *Nat Genet*. 2005; 37:495–500. [PubMed: 15806104]
7. Grimson A, et al. MicroRNA targeting specificity in mammals: determinants beyond seed pairing. *Mol Cell*. 2007; 27:91–105. [PubMed: 17612493]
8. Friedman RC, Farh KK, Burge CB, Bartel DP. Most mammalian mRNAs are conserved targets of microRNAs. *Genome Res*. 2009; 19:92–105. [PubMed: 18955434]
9. Shin C, et al. Expanding the microRNA targeting code: functional sites with centered pairing. *Mol Cell*. 2010; 38:789–802. [PubMed: 20620952]
10. Lim LP, et al. Microarray analysis shows that some microRNAs downregulate large numbers of target mRNAs. *Nature*. 2005; 433:769–73. [PubMed: 15685193]
11. Krutzfeldt J, et al. Silencing of microRNAs in vivo with ‘antagomirs’. *Nature*. 2005; 438:685–9. [PubMed: 16258535]
12. Farh KK, et al. The widespread impact of mammalian microRNAs on mRNA repression and evolution. *Science*. 2005; 310:1817–1821. [PubMed: 16308420]
13. Giraldez AJ, et al. Zebrafish MiR-430 promotes deadenylation and clearance of maternal mRNAs. *Science*. 2006; 312:75–9. [PubMed: 16484454]
14. Nielsen CB, et al. Determinants of targeting by endogenous and exogenous microRNAs and siRNAs. *RNA*. 2007; 13:1894–910. [PubMed: 17872505]
15. Robins H, Li Y, Padgett RW. Incorporating structure to predict microRNA targets. *Proc Natl Acad Sci U S A*. 2005; 102:4006–9. [PubMed: 15738385]
16. Zhao Y, Samal E, Srivastava D. Serum response factor regulates a muscle-specific microRNA that targets *Hand2* during cardiogenesis. *Nature*. 2005; 436:214–20. [PubMed: 15951802]
17. Kertesz M, Iovino N, Unnerstall U, Gaul U, Segal E. The role of site accessibility in microRNA target recognition. *Nat Genet*. 2007; 39:1278–84. [PubMed: 17893677]
18. Long D, et al. Potent effect of target structure on microRNA function. *Nat Struct Mol Biol*. 2007; 14:287–94. [PubMed: 17401373]
19. Hammell M, et al. mirWIP: microRNA target prediction based on microRNA-containing ribonucleoprotein-enriched transcripts. *Nat Methods*. 2008
20. Saetrom P, et al. Distance constraints between microRNA target sites dictate efficacy and cooperativity. *Nucleic Acids Res*. 2007; 35:2333–42. [PubMed: 17389647]
21. Kedde M, et al. RNA-binding protein Dnd1 inhibits microRNA access to target mRNA. *Cell*. 2007; 131:1273–86. [PubMed: 18155131]
22. Ruby JG, et al. Evolution, biogenesis, expression, and target predictions of a substantially expanded set of *Drosophila* microRNAs. *Genome Res*. 2007; 17:1850–64. [PubMed: 17989254]
23. Didiano D, Hobert O. Perfect seed pairing is not a generally reliable predictor for miRNA-target interactions. *Nat Struct Mol Biol*. 2006; 13:849–51. [PubMed: 16921378]
24. Ui-Tei K, Naito Y, Nishi K, Juni A, Saigo K. Thermodynamic stability and Watson-Crick base pairing in the seed duplex are major determinants of the efficiency of the siRNA-based off-target effect. *Nucleic Acids Res*. 2008; 36:7100–9. [PubMed: 18988625]
25. Franco-Zorrilla JM, et al. Target mimicry provides a new mechanism for regulation of microRNA activity. *Nat Genet*. 2007; 39:1033–7. [PubMed: 17643101]
26. Ebert MS, Neilson JR, Sharp PA. MicroRNA sponges: competitive inhibitors of small RNAs in mammalian cells. *Nat Methods*. 2007; 4:721–6. [PubMed: 17694064]
27. Anderson EM, et al. Experimental validation of the importance of seed complement frequency to siRNA specificity. *RNA*. 2008; 14:853–61. [PubMed: 18367722]

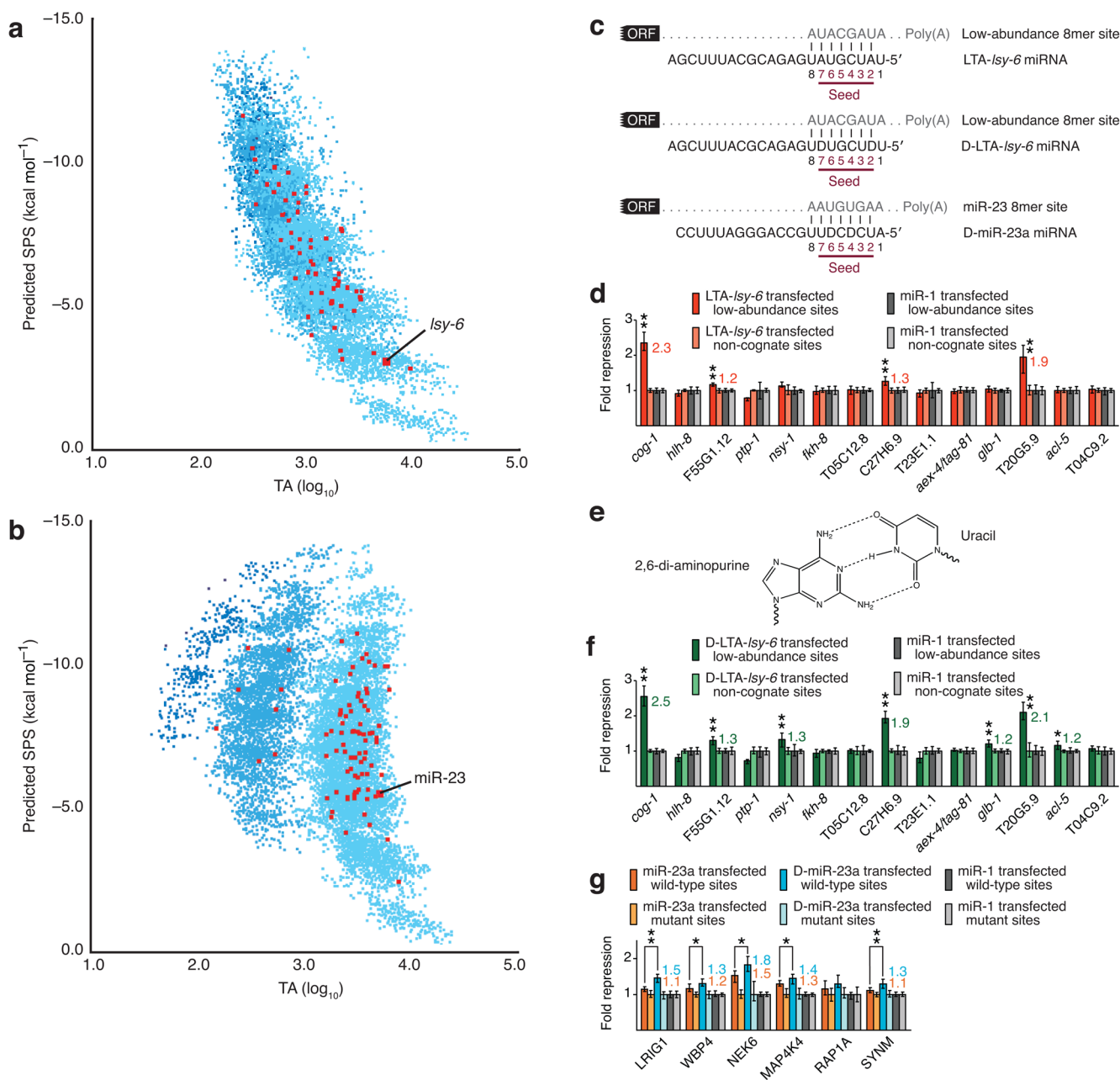
28. Arvey A, Larsson E, Sander C, Leslie CS, Marks DS. Target mRNA abundance dilutes microRNA and siRNA activity. *Mol Syst Biol.* 2010; 6:363. [PubMed: 20404830]
29. Rodriguez A, et al. Requirement of bic/microRNA-155 for normal immune function. *Science.* 2007; 316:608–11. [PubMed: 17463290]
30. Baek D, et al. The impact of microRNAs on protein output. *Nature.* 2008; 455:64–71. [PubMed: 18668037]
31. Bird A. DNA methylation patterns and epigenetic memory. *Genes Dev.* 2002; 16:6–21. [PubMed: 11782440]
32. Xia T, et al. Thermodynamic parameters for an expanded nearest-neighbor model for formation of RNA duplexes with Watson-Crick base pairs. *Biochemistry.* 1998; 37:14719–35. [PubMed: 9778347]
33. Guo H, Ingolia NT, Weissman JS, Bartel DP. Mammalian microRNAs predominantly act to decrease target mRNA levels. *Nature.* 2010; 466:835–40. [PubMed: 20703300]
34. Selbach M, et al. Widespread changes in protein synthesis induced by microRNAs. *Nature.* 2008; 455:58–63. [PubMed: 18668040]
35. Lall S, et al. A genome-wide map of conserved microRNA targets in *C. elegans*. *Curr Biol.* 2006; 16:460–71. [PubMed: 16458514]
36. Jan CH, Friedman RC, Ruby JG, Bartel DP. Formation, regulation and evolution of *Caenorhabditis elegans* 3'UTRs. *Nature.* 2011; 469:97–101. [PubMed: 21085120]
37. Didiano D, Hobert O. Molecular architecture of a miRNA-regulated 3' UTR. *RNA.* 2008; 14:1297–317. [PubMed: 18463285]
38. Huesken D, et al. Design of a genome-wide siRNA library using an artificial neural network. *Nat Biotechnol.* 2005; 23:995–1001. [PubMed: 16025102]
39. Schwarz DS, et al. Asymmetry in the assembly of the RNAi enzyme complex. *Cell.* 2003; 115:199–208. [PubMed: 14567917]
40. Khvorova A, Reynolds A, Jayasena SD. Functional siRNAs and miRNAs exhibit strand bias. *Cell.* 2003; 115:209–16. [PubMed: 14567918]
41. Bartel DP, Chen CZ. Micromanagers of gene expression: the potentially widespread influence of metazoan microRNAs. *Nat Rev Genet.* 2004; 5:396–400. [PubMed: 15143321]
42. Stark A, Brennecke J, Bushati N, Russell RB, Cohen SM. Animal MicroRNAs confer robustness to gene expression and have a significant impact on 3' UTR evolution. *Cell.* 2005; 123:1133–46. [PubMed: 16337999]
43. Seitz H. Redefining microRNA targets. *Curr Biol.* 2009; 19:870–3. [PubMed: 19375315]
44. Ameres SL, Martinez J, Schroeder R. Molecular basis for target RNA recognition and cleavage by human RISC. *Cell.* 2007; 130:101–12. [PubMed: 17632058]
45. Parker JS, Parizotto EA, Wang M, Roe SM, Barford D. Enhancement of the seed-target recognition step in RNA silencing by a PIWI/MID domain protein. *Mol Cell.* 2009; 33:204–14. [PubMed: 19187762]
46. Lewis BP, Shih IH, Jones-Rhoades MW, Bartel DP, Burge CB. Prediction of mammalian microRNA targets. *Cell.* 2003; 115:787–98. [PubMed: 14697198]
47. Pruitt KD, Katz KS, Sicotte H, Maglott DR. Introducing RefSeq and LocusLink: curated human genome resources at the NCBI. *Trends Genet.* 2000; 16:44–7. [PubMed: 10637631]
48. Imanishi T, et al. Integrative annotation of 21,037 human genes validated by full-length cDNA clones. *PLoS Biol.* 2004; 2:e162. [PubMed: 15103394]
49. Lander ES, et al. Initial sequencing and analysis of the human genome. *Nature.* 2001; 409:860–921. [PubMed: 11237011]
50. Kent WJ. BLAT--the BLAST-like alignment tool. *Genome Res.* 2002; 12:656–64. [PubMed: 11932250]
51. Okazaki Y, et al. Analysis of the mouse transcriptome based on functional annotation of 60,770 full-length cDNAs. *Nature.* 2002; 420:563–73. [PubMed: 12466851]
52. Waterston RH, et al. Initial sequencing and comparative analysis of the mouse genome. *Nature.* 2002; 420:520–62. [PubMed: 12466850]

53. Ruby JG, et al. Large-scale sequencing reveals 21U-RNAs and additional microRNAs and endogenous siRNAs in *C. elegans*. *Cell*. 2006; 127:1193–207. [PubMed: 17174894]
54. Griffiths-Jones S, Saini HK, van Dongen S, Enright AJ. miRBase: tools for microRNA genomics. *Nucleic Acids Res*. 2008; 36:D154–8. [PubMed: 17991681]
55. Rhead B, et al. The UCSC Genome Browser database: update 2010. *Nucleic Acids Res*. 2010; 38:D613–9. [PubMed: 19906737]

**Figure 1.**

Increasing SPS while decreasing TA imparted typical targeting proficiency to *Lsy-6* and miR-23 miRNAs. **(a)** Sequences of miRNAs and target sites tested in reporter assays of this figure. Each miRNA was co-transfected with reporter plasmids as a duplex designed to represent the miRNA paired with its miRNA* strand (Supplementary Fig 1a). **(b)** Response of reporters with 3'UTRs of predicted *Lsy-6* targets following co-transfection with *Lsy-6*. As a specificity control, the experiment was also performed using a non-cognate miRNA, miR-1 (grey bars). Geometric means are plotted relative to those of reporters in which the predicted target sites were mutated after also normalizing for the repression observed for miR-1 (grey bars). The mutant sites of this experiment were the cognate sites of Figure 2d. Error bars represent the third largest and third smallest values among 12 replicates from 4 independent experiments. Statistically significant differences in repression by the cognate miRNA compared to that by the non-cognate miRNA are indicated. (* $p < 0.01$, ** $p < 0.001$, Wilcoxon rank-sum test). **(c)** Distribution of predicted SPSs for 7mer-m8 sites of 60 conserved nematode miRNA families³⁶ (Supplementary Table 7). Values were rounded down to the next half-integer unit. **(d)** SPS distribution for 7mer-m8 sites of 87 conserved vertebrate miRNA families⁸ (Supplementary Table 7). **(e)** Distributions of predicted genome TA for 7mer-m8 3'UTR sites of 60 conserved nematode miRNA families (Supplementary Table 7). Values were rounded up to the next tenth of a unit. **(f)** Distributions of predicted genome TA for 7mer-m8 3'UTR sites of 87 conserved vertebrate miRNA families (Supplementary Table 7). **(g)** Response of reporters mutated such that their sites matched the miR-142 seed. The cognate miRNA was the miR-142/*Lsy-6* chimera; non-cognate sites were

lcy-6 sites. Otherwise, as in **b**. **(h)** As in **g**, except showing the response to miR-142 transfection. **(i)** Response of reporters with 3'UTRs of predicted miR-23 targets following co-transfection with miR-23a. Non-cognate sites were for miR-CGCG. Otherwise, as in **b**. **(j)** Response of reporters mutated such that their sites matched the seed of miR-CGCG, which was co-transfected as the cognate miRNA. Non-cognate sites were for miR-23. Otherwise, as in **i**.

**Figure 2.**

Separating the effects of SPS and TA on miRNA targeting proficiency. **(a)** The relationship between predicted SPS and genomic TA for *Isy-6* and the 59 other conserved nematode miRNAs (red squares), and all other heptamers (light blue, blue, dark blue, or purple squares indicating 0, 1, 2, or 3 CpG dinucleotides within the heptamer respectively). TA was defined as the total number of canonical 7–8-nucleotide sites (8mer, 7mer-m8, and 7mer-A1) in annotated 3'UTRs. SPS values were predicted using the respective 7mer-m8 sites. **(b)** The relationship between predicted SPS and TA in human 3'UTRs for miR-23 and the 86 other broadly conserved vertebrate miRNA families (red squares). Otherwise, as in **a**. **(c)** Sequences of miRNAs and target sites tested in reporter assays of this figure. **(d)** Response of reporters with 3'UTRs of predicted *Isy-6* targets mutated such that their sites matched the

seed of LTA-*Isy-6*, which was co-transfected as the cognate miRNA. Non-cognate sites were for *Isy-6*. Otherwise, as in Figure 1b. **(e)** 2,6-di-aminopurine (DAP or D)—uracil base pair. **(f)** Response of reporters used in **d** after co-transfecting D-LTA-*Isy-6* as the cognate miRNA. Otherwise, as in **d**. **(g)** Response of reporters used in Figure 1i after co-transfecting D-miR-23a as the cognate miRNA, alongside results for miR-23a that was repeated in parallel. Otherwise, as in Figure 1i.

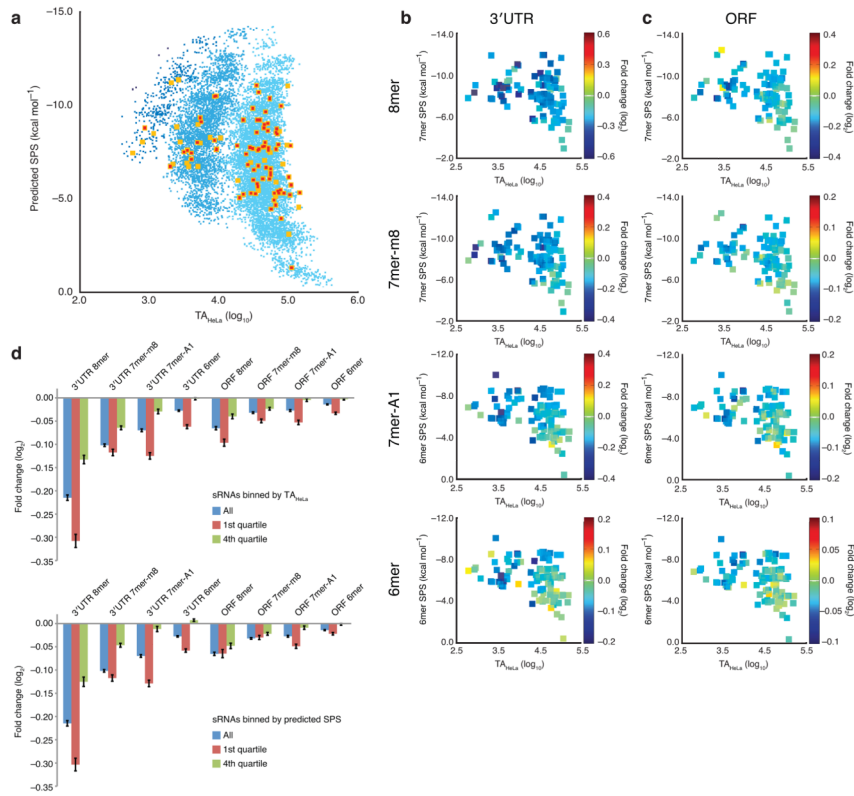


Figure 3. Impact of TA and SPS on sRNA targeting proficiency, as determined using array data. **(a)** Distribution of TA_{HeLa} and predicted SPS for the sRNAs from the 102 array datasets analyzed in this study (orange squares), and sRNAs from datasets that passed the motif-enrichment analysis (red squares). Otherwise, plotted as in Figure 2b. **(b)** Response of expressed mRNAs with a single 3'UTR site to the cognate sRNA, shown with respect to TA_{HeLa} and predicted SPS. Fold-change values are plotted according the key to the right of each plot, comparing mRNAs with a single site of the type indicated (and no additional sites to the cognate sRNA elsewhere in the mRNA) to those with no site to the cognate sRNA; note different scales for different plots. In areas of overlap, mean values are plotted. Correlation coefficients and P values are in Table 1. **(c)** Response of expressed mRNAs with a single ORF site to the cognate sRNA, shown with respect to TA_{HeLa} and predicted SPS. Otherwise, as in **b**. **(d)** Response of mRNAs with the indicated single sites when binning the cognate sRNA by TA_{HeLa} (top panel) or predicted SPS (bottom panel). The key indicates the data considered, with the first quartiles of the top panel comprising data for sRNAs with the lowest TA_{HeLa} and those of the bottom panel comprising data for sRNAs with the strongest predicted SPS. Error bars indicate 95% confidence intervals.

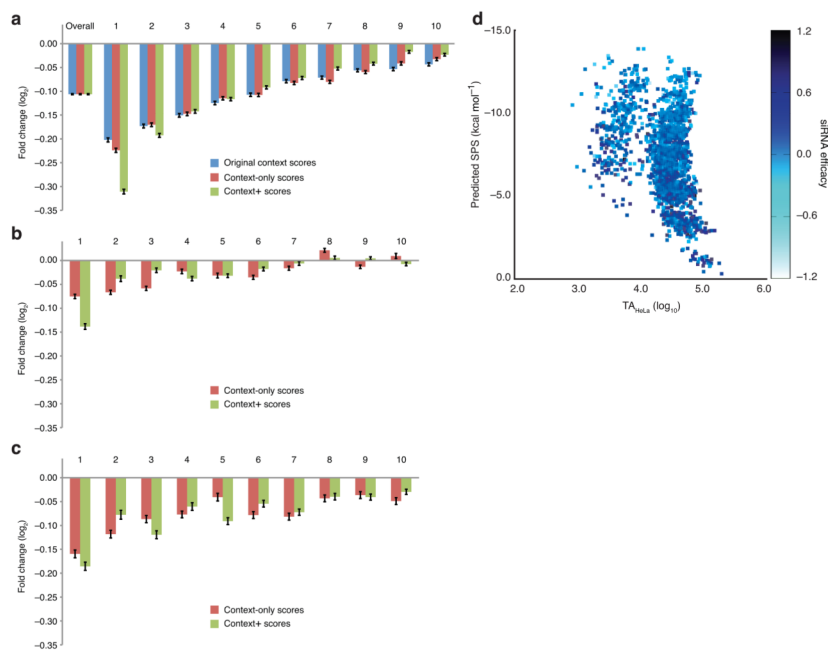


Figure 4. Predictive performance of the context+ model, which considers miRNA or siRNA proficiency in addition to site context. **(a)** Improved predictions for mRNAs with canonical 7–8-nucleotide 3′UTR sites. Predicted interactions between mRNAs and cognate sRNA were distributed into 10 equally populated bins based on total context scores generated using the model indicated (key), with the first bin comprising interactions with the most favorable scores. Plotted for each bin is the mean mRNA change on the arrays (error bars, 95% confidence intervals). **(b)** Prediction of responsive interactions involving mRNAs with only 3′UTR 6mer sites. Otherwise, as in **a**. **(c)** Prediction of responsive interactions involving mRNAs with at least one 8mer ORF site but no 3′UTR sites. Otherwise, as in **a**. **(d)** Impact of TA and SPS on siRNA-directed knock-down of the desired target. Efficacy in luciferase activity knock-down is plotted for 2,431 siRNAs transfected into H1299 cells³⁸. Efficacy is linearly scaled (key), with positive and negative controls having values of 0.900 and 0.354, respectively³⁸.

Table 1

Relationship between mean mRNA repression and either TA or predicted SPS for the indicated site types, as determined from microarray data (Fig. 3b,c)

Site location and type	Multiple linear regression			Simple linear regression		
	Multiple R^2	$T_{A_{HelA}}$	SPS	$T_{A_{HelA}}$	R^2	P value
3' UTR 8mer	0.149	0.0049	0.051	0.115	0.0006	0.076
3' UTR 7mer-m8	0.190	0.0081	0.0047	0.122	0.0003	0.131
3' UTR 7mer-A1	0.335	0.0009	2×10^{-5}	0.196	3×10^{-6}	0.256
3' UTR 6mer	0.177	0.039	0.0025	0.097	0.0014	0.141
ORF 8mer	0.104	0.018	0.14	0.085	0.0030	0.052
ORF 7mer-m8	0.171	0.019	0.0054	0.103	0.0010	0.123
ORF 7mer-A1	0.135	0.010	0.073	0.106	0.0008	0.076
ORF 6mer	0.228	0.010	0.0008	0.133	0.0002	0.174
5' UTR 8mer	0.004	0.75	0.68	0.002	0.64	0.003
5' UTR 7mer-m8	0.003	0.63	0.72	0.002	0.70	0.000
5' UTR 7mer-A1	0.012	0.60	0.49	0.007	0.41	0.009
5' UTR 6mer	0.011	0.97	0.32	0.001	0.74	0.011